

The avocado genome informs deep angiosperm phylogeny, highlights introgressive hybridization, and reveals pathogen-influenced gene space adaptation

Martha Rendón-Anaya^{a,b,1}, Enrique Ibarra-Laclette^{a,c,1}, Alfonso Méndez-Bravo^{a,d}, Tianying Lan^e, Chunfang Zheng^f, Lorenzo Carretero-Paulet^g, Claudia Anahí Perez-Torres^{a,c}, Alejandra Chacón-López^a, Gustavo Hernandez-Guzmán^{a,h,i}, Tien-Hao Chang^e, Kimberly M. Farr^e, W. Brad Barbazuk^j, Srikar Chamala^k, Marek Mutwil^l, Devendra Shivhare^l, David Alvarez-Ponce^m, Neena Mitterⁿ, Alice Haywardⁿ, Stephen Fletcherⁿ, Julio Rozas^{o,p}, Alejandro Sánchez Gracia^{o,p}, David Kuhn^q, Alejandro F. Barrientos-Priego^r, Jarkko Salojärvi^l, Pablo Librado^{s,t}, David Sankoff^l, Alfredo Herrera-Estrella^a, Víctor A. Albert^{e,1,2}, and Luis Herrera-Estrella^{a,u,2}

^aUnidad de Genómica Avanzada/Langebio, Centro de Investigación y de Estudios Avanzados, Irapuato 36821, México; ^bDepartment of Plant Biology, Uppsala BioCenter, Swedish University of Agricultural Sciences, SE-750 07 Uppsala, Sweden; ^cRed de Estudios Moleculares Avanzados, Instituto de Ecología A.C., 91070 Xalapa, México; ^dEscuela Nacional de Estudios Superiores, Laboratorio Nacional de Análisis y Síntesis Ecológica, Universidad Nacional Autónoma de México, 58190 Morelia, México; ^eDepartment of Biological Sciences, University at Buffalo, Buffalo, NY 14260; ^fDepartment of Mathematics and Statistics, University of Ottawa, Ottawa, ON, Canada K1N 6N5; ^gCenter for Plant Systems Biology, Vlaams Instituut voor Biotechnologie (VIB), University of Ghent, 9052 Ghent, Belgium; ^hDepartamento de Alimentos, Universidad de Guanajuato, 36500 Irapuato, México; ⁱDivisión de Ciencias de la Vida, Universidad de Guanajuato, 36500 Irapuato, México; ^jDepartment of Biology, University of Florida, Gainesville, FL 32611; ^kDepartment of Pathology, Immunology and Laboratory Medicine, University of Florida, Gainesville, FL 32610; ^lSchool of Biological Sciences, Nanyang Technological University, Singapore 637551; ^mDepartment of Biology, University of Nevada, Reno, NV 89557; ⁿCentre for Horticultural Science, Queensland Alliance for Agriculture and Food Innovation, The University of Queensland, St. Lucia, QLD 4072, Australia; ^oDepartament de Genètica, Microbiologia i Estadística, Universitat de Barcelona, 08007 Barcelona, Spain; ^pInstitut de Recerca de la Biodiversitat, Universitat de Barcelona, 08007 Barcelona, Spain; ^qSubtropical Horticulture Research Station, Agricultural Research Service, US Department of Agriculture, Miami, FL 33158; ^rPosgrado en Horticultura, Departamento de Fitotecnia, Universidad Autónoma Chapingo, 56230 Texcoco, México; ^sCentre for GeoGenetics, Natural History Museum of Denmark, 1017 Copenhagen, Denmark; ^tLaboratoire d'Anthropobiologie Moléculaire et d'Imagerie de Synthèse, CNRS Unité Mixte de Recherche 5288, Université de Toulouse, Université Paul Sabatier, 31330 Toulouse, France; and ^uDepartment of Plant and Soil Science, Texas Tech University, Lubbock, TX 79409

Contributed by Luis Herrera-Estrella, July 9, 2019 (sent for review December 31, 2018; reviewed by Todd P. Michael and Yves Van de Peer)

The avocado, *Persea americana*, is a fruit crop of immense importance to Mexican agriculture with an increasing demand worldwide. Avocado lies in the anciently diverged magnoliid clade of angiosperms, which has a controversial phylogenetic position relative to eudicots and monocots. We sequenced the nuclear genomes of the Mexican avocado race, *P. americana* var. *drymifolia*, and the most commercially popular hybrid cultivar, Hass, and anchored the latter to chromosomes using a genetic map. Resequencing of Guatemalan and West Indian varieties revealed that ~39% of the Hass genome represents Guatemalan source regions introgressed into a Mexican race background. Some introgressed blocks are extremely large, consistent with the recent origin of the cultivar. The avocado lineage experienced 2 lineage-specific polyploidy events during its evolutionary history. Although gene-tree/species-tree phylogenomic results are inconclusive, syntenic ortholog distances to other species place avocado as sister to the enormous monocot and eudicot lineages combined. Duplicate genes descending from polyploidy augmented the transcription factor diversity of avocado, while tandem duplicates enhanced the secondary metabolism of the species. Phenylpropanoid biosynthesis, known to be elicited by *Colletotrichum* (anthracnose) pathogen infection in avocado, is one enriched function among tandems. Furthermore, transcriptome data show that tandem duplicates are significantly up- and down-regulated in response to anthracnose infection, whereas polyploid duplicates are not, supporting the general view that collections of tandem duplicates contribute evolutionarily recent “tuning knobs” in the genome adaptive landscapes of given species.

avocado genome | angiosperm phylogeny | genome duplications | *Phytophthora* | genome evolution

The avocado, *Persea americana*, is a commercially important tree fruit species in the Lauraceae family, otherwise known for the spices cinnamon, bay leaves, and saffras (gumbo filé) (1). Lauraceae is contained within the early diverging magnoliid lineage of angiosperms, which at about 11,000 total species is minuscule in comparison to the dominant eudicot and monocot

flowering plant lineages, comprising about 285,000 species combined (2). Avocados are a vital crop for Mexico, from which almost 50% of all avocado exports originate, valued at

Significance

The avocado is a nutritious, economically important fruit species that occupies an unresolved position near the earliest evolutionary branchings of flowering plants. Our nuclear genome sequences of Mexican and Hass variety avocados inform ancient evolutionary relationships and genome doublings and the admixed nature of Hass and provide a look at how pathogen interactions have shaped the avocado's more recent genomic evolutionary history.

Author contributions: N.M., A.H.-E., V.A.A., and L.H.-E. designed research; M.R.-A., E.I.-L., A.M.-B., C.A.P.-T., A.C.-L., G.H.-G., N.M., A.H., D.K., A.F.B.-P., D. Sankoff, and V.A.A. performed research; N.M., D.K., A.F.B.-P., and L.H.-E. contributed new reagents/analytic tools; M.R.-A., E.I.-L., A.M.-B., T.L., C.Z., L.C.-P., C.A.P.-T., A.C.-L., G.H.-G., T.-H.C., K.M.F., W.B.B., S.C., M.M., D. Shivhare, D.A.-P., A.H., S.F., J.R., A.S.G., J.S., P.L., D. Sankoff, A.H.-E., V.A.A., and L.H.-E. analyzed data; and M.R.-A., E.I.-L., A.H.-E., V.A.A., and L.H.-E. wrote the paper.

Reviewers: T.P.M., J. Craig Venter Institute; and Y.V.D.P., Ghent University.

The authors declare no conflict of interest.

This open access article is distributed under Creative Commons Attribution-NonCommercial-NoDerivatives License 4.0 (CC BY-NC-ND).

Data deposition: Bioproject: PRJNA508502. Biosamples: SAMN10523735, SAMN10523720, SAMN10523736, SAMN10523738, SAMN10523739, SAMN10523746, SAMN10523747, SAMN10523748, SAMN10523749, SAMN10523750, SAMN10523752, SAMN10523753, and SAMN10523756. SRA submission: SUB4878870. Whole Genome Shotgun projects have been deposited at DDBJ/ENA/GenBank (accession nos. SDXN000000000 and SDSS000000000). The versions described in this paper are version SDXN010000000 and SDSS010000000 (*P. americana* var. *drymifolia* and *P. americana* cultivar Hass, respectively). The genome assemblies and annotations are available at <https://genomevolution.org/CoGe/SearchResults.pl?ts=29305&p=genome> and <https://genomevolution.org/CoGe/SearchResults.pl?ts=29302&p=genome> (*P. americana* var. *drymifolia* and *P. americana* cultivar Hass, respectively).

¹M.R.-A. and E.I.-L. contributed equally to this work.

²To whom correspondence may be addressed. Email: vaalbert@buffalo.edu or lherrerae@cinvestav.mx.

This article contains supporting information online at www.pnas.org/lookup/suppl/doi:10.1073/pnas.1822129116/-DCSupplemental.

Published online August 6, 2019.

about \$2.5 billion US dollars.* Although the avocado has an ancient cultivation history in Mexico and Central to South America (5), its extreme worldwide popularity as an oily, nutty-flavored fruit with highly beneficial nutritional properties dates mainly from the early 20th century (6). Cultivated avocados occur in 3 landraces with possibly independent cultivation origins that reflect their current distribution: the Mexican, Guatemalan, and West Indian varieties (6). The principal industrial avocado cultivar is known as Hass, after the grower who first patented it in 1935. Hass represents a hybrid between the Guatemalan and Mexican races, but its precise breeding history is unknown (6, 7). Here, we generate and analyze the complete genome sequences of a Hass individual and a representative of the highland Mexican landrace, *Persea americana* var. *drymifolia*. We also study genome resequencing data for other Mexican individuals, as well as Guatemalan and West Indian accessions. We use these data to study the admixed origin of the Hass cultivar and demonstrate its racewise parentage more precisely. We evaluate the phylogenetic origin of avocado among angiosperms and provide information on avocado's unique polyploid ancestry. The adaptive landscape of the avocado genome in terms of its duplicate gene functional diversity was also explored. We further evaluate gene expression patterns during the defense response of Hass avocado to anthracnose disease and how this is partitioned by gene duplication mechanisms.

Results and Discussion

Plant Material, Genome Assembly, and Annotation. Due to growing market demand, 90% of cultivated avocado corresponds to the cultivar Hass, which in Mexico is commonly grafted on Mexican race (*P. americana* var. *drymifolia*) rootstock (6). This practice makes it possible to maintain high productivity as the indigenous race is well-adapted to Mexican highland soils. The Hass cultivar and Mexican race were chosen to generate reference genomes (*SI Appendix*, section 1). Additionally, to explore the genetic diversity available in avocado, we resequenced representative individuals from the 3 avocado botanical varieties (vars. *drymifolia*, *guatemalensis*, and *americana*), including the disease-resistant rootstock Velvick (8), an additional Hass specimen and the early flowering/fruitlet Hass somatic mutant Carmen Hass cultivar [otherwise known as Mendez No. 1 (6, 9)], as well as wild avocados of the West Indian variety (*P. americana* var. *costaricensis*). *Persea shiedeana* (the edible coyo), a species relatively closely related to *P. americana* (10), was also included (*SI Appendix*, Tables S1 and S2).

De novo and evidence-directed annotation revealed a similar number of protein coding genes in each genome: 22,441 from the Mexican race and 24,616 from Hass (Table 1, *SI Appendix*, section 2, and *Datasets S2* and *S3*). We next used the Benchmarking Universal Single-Copy Orthologs (BUSCO) software to estimate the presence of 1,440 conserved embryophyte single-copy genes (11) in the annotations, leading to estimated completeness percentages of 85% and 86.3% for Hass and Mexican avocado, respectively (Table 1). The Mexican race was sequenced using the short-read, high-coverage Illumina sequencing platform, while the Hass genome was sequenced using the long-read Pacific Biosciences sequencing technology. Given the similar BUSCO scores, we used the larger Hass genome assembly for downstream single-nucleotide polymorphism (SNP) calling, as PacBio technology lowers the probability of contig misassembly and permits incorporation of substantially more repetitive DNA sequence and genes lying within it into the assembled genome, which might have otherwise been missed.

We also anchored the Hass genome to an avocado genetic map (12). Two large mapping populations of 1,339 trees were genotyped with 5,050 SNP markers from transcribed genes, and the resulting map was used to order the Hass scaffolds into 12 linkage groups, matching the avocado haploid chromosome number (see, e.g., chromosome 4, Fig. 24). The total length of the anchored genome accounts for 46.2% of the Hass assembly and represents 915 scaffolds, 361 of which could be oriented (*SI Appendix*, section 1.5).

SNPs, Population Structure, and the Parentage of Hass. To study avocado from a population genomic perspective, we resequenced accessions of different races and cultivars and mapped the reads against the Hass reference genome assembly (*SI Appendix*, Table S2). The estimated depth of coverage ranged from 3.3 to 39×, with breadth of coverage between 70 and 92% (*SI Appendix*, section 3.2). Given the uneven sequencing coverage, we used ANGSD to call SNPs across the entire (unanchored) genome assembly, followed by a stringent pruning based on per-site depth, minor allele frequencies, and linkage disequilibrium, that resulted in 179,029 high-quality SNP variants. Phylogenetic, principal component, and identity-by-state (IBS) analyses derived from this dataset (Fig. 14 and *SI Appendix*, section 4) cluster the samples belonging to the Hass cultivar and Guatemalan variety into 2 groups as expected according to their genetic background. Principal component analysis of genome-wide SNPs showed relative uniformity in Costa Rican/West Indian/Guatemalan group but strong heterogeneity within the Mexican subpopulation, wherein the unusual accession Tiny Charly is a divergent sample (*SI Appendix*, Fig. S15). SNPhylo (13) results reflected the poor fit of the SNP data to a bifurcating tree by embedding the hybrid Hass within an otherwise Mexican clade, 1 known parent of this hybrid cultivar (*SI Appendix*, Fig. S13). Furthermore, in that lineage's sister group, Guatemalan accessions were derived within an otherwise Costa Rican/West Indian lineage, suggesting an admixed origin involving Guatemalan and other sources. Phylogenetic patterns generated from chromosome-wise SNP subsets (based only on contigs anchored to chromosomes) recapitulated these relationships for 7 of avocado's 12 chromosomes, whereas 1 chromosome supported Hass to be sister to the Costa Rican/West Indian lineage, perhaps reflective of chromosomal differences in the admixture proportions of this hybrid cultivar (*SI Appendix*, Fig. S14 and *Dataset S6*). Furthermore, IBS clustering placed Hass intermediate between the Guatemalan and Mexican subpopulations, agreeing with the hybrid nature of this variety (*SI Appendix*, Fig. S16).

To account for further evidence of admixture in the Hass reference genome, we used NGSAdmix (14) modeling different possible numbers of source populations ($K = 1$ to 6) (*SI Appendix*, section 5 and Fig. S17). The Akaike information criterion (AIC) indicated $K = 1$ as the preferred model, reflecting poor population structuring within avocado as a whole. However, since we know Hass is admixed a priori, we chose the smallest (most parsimonious) K for which Hass admixture appears ($K = 3$). This criterion predicts the following 3 populations: 1) *P. shiedeana*, 2) the West Indian plus the Guatemalan varieties, and the 3) Mexican accessions (Fig. 1B). Combining the IBS and NGSAdmix observations, we specifically calculated the contribution of Guatemalan and Mexican backgrounds into the Hass subpopulation. EIGMIX (15) revealed that the greatest admixture proportion, 61%, stemmed from the Mexican race (*SI Appendix*, Fig. S18 and Table S8).

Although based on ~46% anchoring of scaffolds to chromosomes, we investigated chromosomewise signatures of admixture in the Hass genome (*SI Appendix*, section 5.2). We calculated the \hat{f}_D , \hat{f}_{DM} , and d_{XY} estimators of introgression and divergence (*SI Appendix*, Fig. S19 and *Dataset S7*) according to Martin et al.

*Based on information taken from refs. 3 and 4.

Table 1. General statistics of the avocado assemblies and their annotations

Metrics	<i>P. americana</i> assembly	
	Var. <i>drymifolia</i>	Hass cultivar
No. of contigs	99,957	8,135
Total length of contigs, bp	668,137,248	912,697,600
No. of scaffolds	42,722	—
Total length of scaffolds, bp	823,419,498	—
Longest contig/scaffold, bp	254,240/4,610,966	2,811,280/—
Mean contig/scaffold length, bp	6,684/19,274	112,194/—
N50 contig/scaffold length, bp	11,724/323,854	296,371/—
Assembly in scaffolded contigs, %	87.6	0
Assembly in unscaffolded contigs, %	12.4	100
Protein coding genes (% BUSCO completeness)	22,441 (86.3%)	24,616 (85%)

(16) in nonoverlapping 100-kb windows, controlling the directionality of gene flow from the Guatemalan race into Hass versus the Mexican race into Hass, setting *P. schiedeana* as the outgroup and leaving Tiny Charly out of the Mexican subpopulation to avoid the bias this divergent accession could introduce into calculations (Fig. 2B). Genomic regions that behave as \hat{f}_{dM} outliers can be distinguished as introgressed from ancestral variation if the absolute genetic distance d_{XY} is also reduced between donor (P_3) and receptor (P_2). In the presence of gene flow, genomic windows coalesce more recently than the lineage split, so the magnitude of reduction in $P_2 - P_3 d_{XY}$ is greater than in the case where recombination and hybridization are absent. We evaluated several \hat{f}_{dM} cutoffs (Q50, 75, and 90; *SI Appendix, Fig. S20*) and observed a remarkable reduction of genetic divergence in the scenario where gene flow occurs from the Guatemalan race into Hass. Considering those blocks with $\hat{f}_{dM}[\text{Guat-Hass}] > 0.174$ (Q50), $d_{XY}[\text{Guat-Hass}] < 0.113$ (mean divergence between subpopulations) and $\hat{f}_{dM}[\text{Drym-Hass}] < 0.114$ (Q50), we were able to define 840 high-confidence regions of

Guatemalan origin across the 12 chromosomes (Fig. 2, *SI Appendix, section 5.2* and Figs. S21 and S23–S34). Chromosome 4 illustrates these analyses well, demonstrating that a huge Guatemalan block, which could encompass an entire chromosome arm, is present in the Hass genome (Fig. 24). The length of this Guatemalan-derived block, uninterrupted by recombination, reflects the extremely recent hybrid origin of the cultivar.

We also calculated the level of nucleotide diversity [π (17, 18)] in each population (Mexican, Guatemalan, and Hass), the F_{ST} index (19) to determine regions of high differentiation between varieties, and Tajima's D (20) in order to evaluate any deviations from neutral evolution (*SI Appendix, section 5.3* and *Dataset S7*). We observed that Hass has the lowest nucleotide diversity ($\pi = 0.06$) and very high Tajima's D in all chromosomes (genomic average of 1.5), as expected for individuals derived from a recent founder event and clonally propagated; these values contrast with the low, positive Tajima's D values in the Mexican and Guatemalan populations (genomic averages of 0.19 and 0.11, respectively; *SI Appendix, Fig. S22*). In the case of chromosome 4, the F_{ST} index between the Mexican race and Hass corroborates our

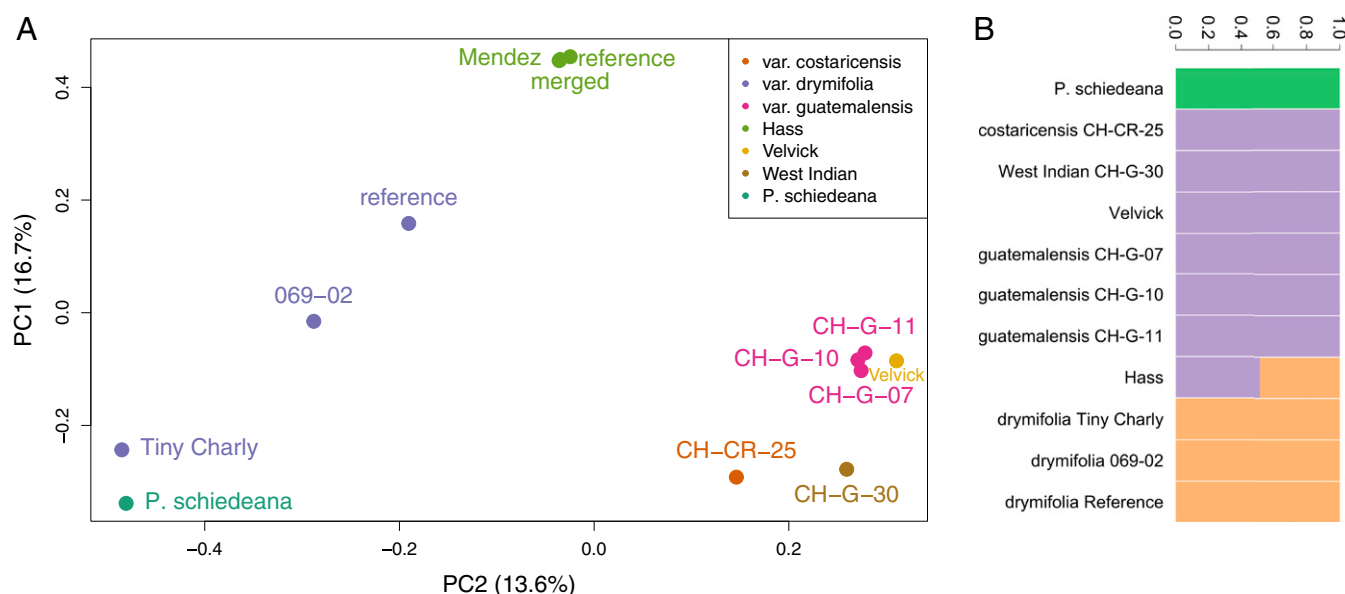


Fig. 1. Population genomic structure of avocado. (A) Principal component analysis (PCA) of genome-wide SNPs reveals population groupings among races and varieties. The Guatemalan and West Indian/Costa Rican accessions are closely related, while the Mexican (*P. americana* var. *drymifolia*) specimens are more diverse, with the unusual individual Tiny Charly drawn toward the outgroup species *P. schiedeana* by PC2. Hass and its sport Mendez are tightly clustered and intermediate between Mexican and Guatemalan and West Indian/Costa Rican on PC2. (B) NGSAdmix analysis reveals similar population structure at $K = 3$. The *P. schiedeana* outgroup is distinct, and the Hass reference genome is revealed to be admixed between Guatemalan–West Indian and Mexican source populations, the Mexican source clearly contributing greater than 50%.

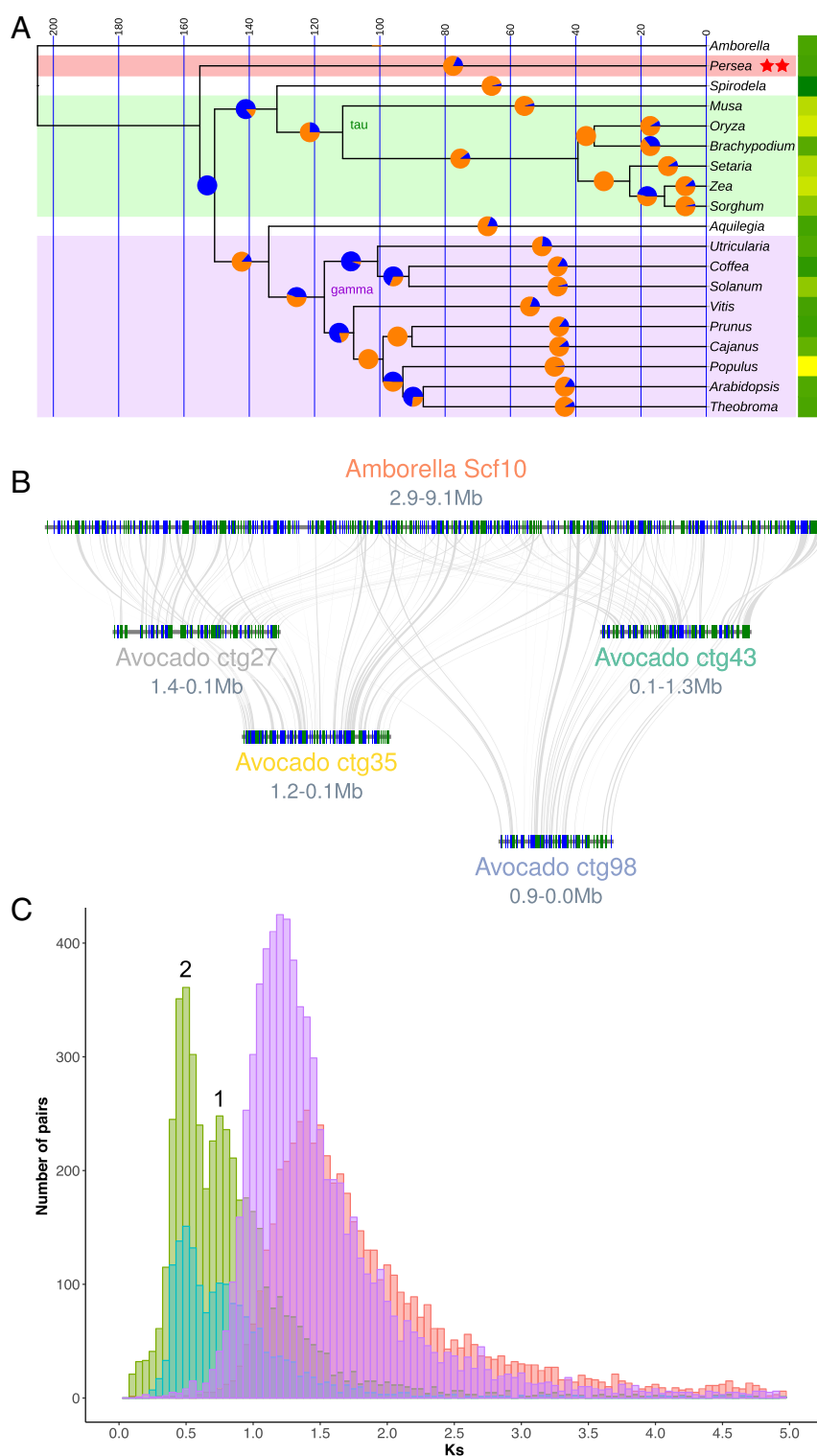


Fig. 3. Phylogenomic and whole-genome duplication history of avocado. (A) An ultrametric time tree based on universally present single-copy protein sequences depicts 1 of 3 common resolutions of *Persea* (Magnoliidae) relationships to other flowering plants. This topology, showing avocado sister to monocots plus eudicots, mirrors phylogenetic relationships derived from syntenic distances. Here, the split time between the last common ancestor of avocado and the monocot/eudicot crown group is less than 4 million y. Pie charts at 50% positions on branches show proportions of gene gains (orange) versus losses (blue) as determined by BadiRate's birth-death-innovation model. Yellow-green (greater-lesser) heat map to the right of the tree depicts relative numbers of genes in the modern genomes. Syntenic analysis revealed 2 independent WGD events (red stars) during avocado's evolutionary history. (B) Hass avocado (bottom 4 genomic blocks) shows 4:1 intercalated syntenic relationships with *Amborella* (upper block). (C) Syntenic homologs in avocado show a bimodal K_s distribution suggestive of 2 polyploidy events (numbered 1 and 2; cyan: Hass:Hass paralogs; green: Hass:*drymifolia* homologs) following the split between magnoliids and *Amborella* (red syntenic homologs). These events postdate the species split between *Vitis* and avocado (purple syntenic homologs) and so are independent of the gamma triplication that underlies *Vitis*.

using 2 data forms: coding sequence alignments and modal distances within large collections of syntenic orthologs between species pairs (*SI Appendix, section 7*).

Single-copy gene families [presumed unambiguous orthologs, those that returned to single copy following duplicate deletions after the various polyploidy events in flowering plant history (27)] were retrieved from orthogroup classification of 19 angiosperm proteomes, including those of avocado, *Amborella*, and representatives of monocots and eudicots (*SI Appendix, section 3.1* and *Dataset S4*). Phylogenetic trees based on 176 stringently filtered single-copy gene alignments (*SI Appendix, section 7.1* and *Datasets S8* and *S9*) gave different results for amino acid versus inferred codon data. Based on protein sequences, avocado was resolved as sister to monocots plus eudicots (i.e., branching before their divergence from each other; cf. refs. 28 and 29), whereas from coding sequences avocado was placed as sister to monocots only (cf. ref. 30) (*SI Appendix, Figs. S40* and *S41*, respectively). In a different analysis we included *Gnetum* (a gymnosperm) and *Selaginella* (a nonseed plant) in orthogroup classification to generate a rooted species tree from all gene trees (4,694) that contained one or more (i.e., paralogous) gene copies from all species (*SI Appendix, section 7.2*). Here, avocado was resolved as sister to eudicots only (*SI Appendix, Fig. S42*), a result similarly found in transcriptome-based analyses of large numbers of species (26, 31). In an altogether different approach (32, 33), we generated a neighbor-joining tree based on modal dissimilarity scores from thousands of syntenically validated ortholog pairs generated by the SynMap function on the CoGe platform (21) (*SI Appendix, section 7.3*). Here, avocado was again placed as sister to monocots plus eudicots, as in Fig. 3A (*SI Appendix, Fig. S44*).

Apparently, the early branching orders of the angiosperms are extremely difficult to determine using protein coding sequences. This problem is due in part to sequence parallelism/reversal over deep time, limitations in taxon sampling (including unknown extinctions), biases in sequence-based ortholog versus paralog determination, but clearly also to the relatively coincident branching times of the species involved (see figure 6 of ref. 34 and also below). Rapid species divergences can lead to real gene-tree/species-tree discordances through enhanced occurrence of incomplete lineage sorting (ILS), wherein polymorphic allele states in ancestral populations do not have enough time to fix according to the species tree (35–37).

In an experimental approach to the problem, we further investigated the possible role of ILS using gene family turnover analysis as incorporated in BadiRate (38) (*SI Appendix, section 7.4*). Trees with the 3 alternative placements of avocado were converted into time-calibrated ultrametric trees, and the likelihoods of duplicate gains versus losses were evaluated under 4 different branch models (*SI Appendix, section 7.4*). The AIC clearly favored free-rates (FR) models, supporting heterogeneous rates of multigene family evolution across lineages (*Dataset S10*). Interestingly, such uneven rates of gene turnover cannot be entirely explained by lineage-specific WGD/whole-genome triplication (WGT) events, given that FR models fit multigene family data better than WGD/WGT models alone. Additionally, allowing turnover rates to vary in each short branch (<10 My) also improved likelihood and AIC values, although the fit was still worse than under the FR model (*Dataset S10*). That FR models fit gene count data significantly better could be explained by their flexibility to accommodate variation that is not explicitly accounted for by current turnover models, such as gene copy variation within species. Intraspecific variation, segregating in an ancestral population, can be inherited differently by 2 splitting lineages, which will thus start diverging with a significant fraction of differentiation. This predicts that divergence will be inflated for short branches, and that this bias will become negligible as divergence times increase, because its relative contribution to the total divergence tends to be

comparatively small over time (39, 40). We observe a correlation between turnover rates and branch lengths at the multigene family level (*SI Appendix, Fig. S46*), suggesting pervasive copy number variation (CNV) in the ancestral species, possibly exacerbated by WGD and subsequent fractionation processes. Short phylogenetic branches, representing rapid speciation events, increase the incidence of ILS in phylogeny reconstruction since extinctions of alternative duplicate copies within ancestral populations (e.g., unfixed CNVs) further break up branches that are nearly time-coincident already (41). According to BadiRate estimates, the temporal impact of ILS on turnover rates extended well beyond 10 Mya, a time frame exceeding the branch length of the lineage that existed immediately prior to avocado divergence from other species, which varied in age from only 7.4 to as little as 3.8 My (Fig. 3A and *SI Appendix, Table S11* and *Figs. S46* and *S47*). This implies that the 3 different placements of avocado among angiosperms may be impossible to discriminate among for purely biological reasons (cf. ref. 42). Yet, 1 of the 3 different tree topologies was preferred based on AIC contrasts under the FR model: the topology wherein magnoliids are sister to monocots plus eudicots (Fig. 3A and *SI Appendix, Fig. S47*).

Functional Enrichments in Duplicate Gene Space. Duplicate gene collections within plant genomes mainly derive from 2 processes, local and ongoing tandem duplication events, many of which may be recent, and global and often ancient polyploidy events wherein entire gene complements are duplicated (43). Subfunctionalization and/or neofunctionalization of duplicate gene copies (44) results in retained descendants of duplication events that have differentially escaped the otherwise usual fate of duplicates—pseudogenization—through functional divergence. Tandem duplication is problematic for genes that are part of dosage-sensitive transcriptional regulatory networks, or for genes that code for parts of multiprotein complexes (45). Such functions are more likely to remain among the surviving duplicate complements stemming from precisely dosage-balancing polyploidy events (46). On the other hand, dosage-responsive functions such as secondary metabolism (including biochemical pathway addition) are among those most likely to survive as sub- or neofunctionalized tandem duplicates (45). These patterns have been repeatedly observed among plant genomes, wherein secondary metabolic function is most prevalent among tandems, and transcriptional function is enriched among polyploid duplicates (e.g., refs. 46 and 47). The avocado genome provides no exception to this rule; we identified precisely these overrepresentation patterns among Gene Ontology (GO) and Kyoto Encyclopedia of Genes and Genomes (KEGG) categories for these different classes of gene duplicates, separated using the CoGe platform (*SI Appendix, section 8*). Among 2,433 total polyploid duplicates, “regulation of transcription, DNA-templated” was significantly overrepresented by 352 genes (*Dataset S12*). Enriched functions among tandem duplicates was highly illustrative of the secondary metabolic landscape particular to avocado (*Dataset S12*). We show that “phenylpropanoid biosynthesis” and closely related KEGG pathways (*Dataset S13*) are significantly enriched among tandem duplicates ($P = 2.08\text{e-}08$; Fisher’s exact test, Bonferroni-corrected). This functional enrichment in a long-lived tree may have evolved in response to pathogen infection, including *Colletotrichum* (anthracnose) and *Phytophthora cinnamomi* (avocado root rot), both of which are reported to activate the phenylpropanoid biosynthetic pathways in avocado (48–50). Several GO functional enrichments among avocado tandems (for example, “1,3-beta-D-glucan synthase activity” and “regulation of cell shape”; $P = 1.64\text{e-}05$ and 0.00258, respectively; Fisher’s exact test, Bonferroni-corrected) relate to callose synthase activity (51, 52), a recently discovered avocado defense mechanism against *P. cinnamomi* (53). Other significantly enriched GOs include

“phenylpropanoid metabolic process,” “lignin biosynthetic process,” and “UDP-glycosyltransferase activity” ($P = 0.00142$, 7.36×10^{-7} and 5.16×10^{-7} , respectively; Fisher’s exact test, Bonferroni-corrected), categories directly or closely related to phenylpropanoid biosynthesis (54, 55). The lignin functional enrichment, for example, includes diverse tandemly duplicated genes involved in many pathway-interrelated processes, including homologs of both biosynthetic and regulatory genes encoding HYDROXYCINNAMOYL-COA SHIKIMATE/QUINATE HYDROXYCINNAMOYL TRANSFERASE (HCT), CINNAMYL ALCOHOL DEHYDROGENASE 5 (CAD5), LACCASE 17 (LAC17), CAFFEATE O-METHYLTRANSFERASE 1 (COMT1), PEROXIDASE 52 (PRX52), NAC DOMAIN CONTAINING PROTEIN 12 (NAC012), and NAC SECONDARY WALL THICKENING PROMOTING FACTOR 1 (NST1). As could be expected from the above, the GOs “defense response” and “defense response to fungus” are significantly enriched among tandem duplicates ($P = 0.000165$ and 0.0167 , respectively; Fisher’s exact test, Bonferroni-corrected), as has been discovered for other plant genomes, and involving many different gene families and responses. Tandem *O*-methyltransferases homologous to COMT1 may also contribute to synthesis of the phenylpropanoid derivative and insecticide estragole (56), which is largely responsible for the anise-like leaf scent and fruit taste of many avocado cultivars, particularly of the Mexican race (57). Another relevant enriched GO category among tandems is “ethylene-activated signaling pathway” ($P = 0.000463$; Fisher’s exact test, Bonferroni-corrected), which annotates many different transcription factor duplicates. Ethylene signaling factors such as ERF1 (represented by 2 homologs) are heavily involved in pathogen-induced responses, including to infection by *Colletotrichum* and other necrotrophic fungi (58–61). Also identified are 3 homologs of EIN3, a transcription factor that initiates downstream ethylene responses, including fruit ripening (62). Avocado fruit matures on the tree in a process that involves ethylene synthesis and signaling, while it does not ripen until harvested—a desirable trait that allows growers to delay harvesting for several months (63).

Given the ancient derivation of avocado’s retained polyploid duplicates, most tandem duplicates in the genome are expected to be of more recent origin, having been generated by ongoing gene birth–death–innovation processes that operate in all eukaryotic genomes. As such, sub- or neofunctionalized tandem duplicates that survive the usual fate of duplicated genes—pseudogenization—should be enriched in functions that fine-tune a given species’ recent selective environment. In the case of avocado, response to fungal pathogens is precisely reflected in its tandemly duplicated gene complement.

Differential Expression of Tandem versus Polyploid Duplicates. Following our prediction that many tandem duplicates fixed in the avocado genome may have evolved under relatively recent pathogen pressure, we examined differential expression of Hass genes after treatment with the anthracnose causal agent (64) (*SI Appendix, section 9*). Hass transcriptome reads for untreated control versus pathogen-treated were mapped to Hass gene models using Kallisto (65), normalized to transcript-per-million values and thresholded by identifying genes with treatment/control log₂ fold change outside of the $[2, -2]$ interval. Tandems were significantly enriched among up-regulated ($P = 3.536 \times 10^{-9}$; Fisher’s exact test) and down-regulated genes ($P = 7.274 \times 10^{-7}$), whereas polyploid duplicates did not show enrichment (*SI Appendix, section 9*). We interpret these results to indicate that tandem duplicates are the most dynamic component of the avocado duplicate gene space under pathogen treatment.

We also examined functional enrichments for up- versus down-regulated tandem duplicates (*Dataset S16*). The only significantly enriched category was xyloglucan:xyloglucosyl transferase activity

($P = 0.038984$; Fisher’s exact test, Bonferroni-corrected). Among genes with this annotation were 4 homologs of XYLOGLUCAN ENDOTRANSGLUCOSYLASE/HYDROLASE 22 [*XTH22*; also known as *TOUCH 4 (TCH4)* (66)]. *XTH22* and similar genes encoding cell-wall-modifying proteins have been shown to up- or down-regulate after Citrus Huanglongbing infection (67), whitefly infestation (65), and herbivore (68) or mechanical stimulation (69), the latter provoking a *Botrytis*-protective response. In a different pathogen response, up-regulation of *XTH22* occurs in concert with pectin digestion in *Pseudomonas*-sensitive *Arabidopsis* lines that overexpress *IDA-LIKE 6 [IDL6]* (70)].

Conclusions

Our genomes of Mexican and Hass avocados provide the requisite resources for genome-wide association studies to identify important traits among natural avocado genetic diversity present in Mesoamerica, to develop genome-assisted breeding and genetic modification efforts crucial for the improvement of this long-life-cycle crop, to fight threatening avocado diseases, and to optimize growth and desirable phenotypic traits. We anchored almost half of the sequenced Hass genome to a genetic map, providing linkage information for genetic variation on 12 chromosomes. We resequenced 10 genomes representing small populations of Guatemalan, West Indian, Mexican, and Hass-related cultivars—and the genome of the closely related species *P. schiedeana*—in order to call SNPs and study genetic diversity among these chromosomes. Analyses of admixture and introgression clearly highlighted the hybrid origin of Hass avocado, pointed to its Mexican and Guatemalan progenitor races, and showed Hass to contain Guatemalan introgression in approximately one-third of its genome. Introgressed blocks of chromosome arm size matched expectation based on Hass’s recent (20th century) origin. We uncovered 2 ancient polyploidy events that occurred in the lineage leading to avocado and conclude that these were independent from genome duplications or triplications known to have occurred in other angiosperm clades. We contributed to solving the problem of magnoliid phylogenetic relationships to other major angiosperm clades by showing that thousands of syntenic orthologs among 14 species support an arrangement wherein the magnoliid clade branched off before the split between monocots and eudicots. However, this resolution is tentative, with coding sequence phylogenomics inconclusive and gene family birth/death analysis suggesting appreciable duplicate gene turnover—and therefore enhanced possibility for ILS—during what appears to have been a nearly coincident radiation of the major angiosperm clades. We also studied the adaptive landscape of the avocado genome through functional enrichment analyses of its mechanistically distinct duplicate gene collections, that is, tandem versus polyploid duplicates. Tandem duplicates were enriched with many potentially important metabolic responses that may include relatively recent adaptation against fungal pathogens. In contrast, ancient polyploid duplicates, which originated in 2 distinct waves, were enriched with transcriptional regulatory functions reflective of core physiological and developmental processes. We discovered that tandem duplicates were more dynamically transcribed following anthracnose infection, and that some of the up-regulated genes could be related to defense responses. In sum, our work paves the way for genomics-assisted avocado improvement (1).

Data Availability. Bioproject: PRJNA508502. Biosamples: SAMN10523735, SAMN10523720, SAMN10523736, SAMN10523738, SAMN10523739, SAMN10523746, SAMN10523747, SAMN10523748, SAMN10523749, SAMN10523750, SAMN10523752, SAMN10523753, and SAMN10523756. SRA submission: SUB4878870. Whole Genome Shotgun projects have been deposited at DDBJ/ENA/GenBank under the accession nos. SDXN000000000 and SDSS000000000. The versions described in this paper are versions

SDXN0100000 and SDSS0100000 (*P. americana* var. *drymifolia* and *P. americana* cultivar Hass, respectively). The genome assemblies and annotations are available at <https://genomeevolution.org/CoGe/SearchResults.pl?s=29305&p=genome> and <https://genomeevolution.org/coGe/SearchResults.pl?s=29302&p=genome> (*P. americana* var. *drymifolia* and *P. americana* cultivar Hass, respectively).

Materials and Methods

P. americana var. *drymifolia* was obtained from the germplasm bank of the Instituto Nacional de Investigaciones Forestales y Agropecuarias in Uruapan and the Hass and Carmen Hass cultivars were collected from a commercial orchard in Tingambato, both in Michoacán, Mexico. The remaining resequenced accessions were obtained from the Fundación Salvador Sánchez Colín germplasm bank located at La Cruz Experimental Center at Coatepec Harinas in the state of Mexico. The Velvick rootstock was provided by the University of Queensland, Australia. DNA was extracted from young leaves of single individuals for all cultivars sequenced. For the reference genome of the Hass cultivar, high-quality megabase-sized DNA was submitted to the

National Center for Genome Resources for PacBio single-molecule real-time sequencing. A *P. americana* var. *drymifolia* reference individual was sequenced using different fragment-size libraries (~0.5, 1, 3, 5, or 8 kb). For detailed information about assembly, annotation, and other bioinformatic analysis see *SI Appendix*.

ACKNOWLEDGMENTS. This project was funded in large part by Grant 00126261 from the Secretaría de Agricultura, Ganadería, Recursos Pesqueros y Alimentos/Consejo Nacional de Ciencia y Tecnología sectorial program to L.H.-E.; Grant 05-2018 from the Governor University Research Initiative program from the state of Texas; Howard Hughes Medical Institute Grant 55005946 to L.H.-E.; Grants 0922742 and 1442190 to V.A.A., N.M., and A.H. from the National Science Foundation; Horticulture Innovation Australia Ltd; and the Australian Bureau of Agricultural and Resource Economics and Sciences. We thank the Fundación Salvador Sánchez Colín—Centro de Investigaciones Científicas y Tecnológicas de Aguacate en el Estado de México, S.C. for providing avocado specimens. We also thank Araceli Fernandez and Emanuel Villafan, administrators of the high-performance computing systems at Laboratorio Nacional de Genómica para la Biodiversidad and Instituto Nacional de Ecología, respectively.

1. A. S. Chanderbali *et al.*, *Persea americana* (avocado): Bringing ancient flowers to fruit in the genomics era. *BioEssays* **30**, 386–396 (2008).
2. M. J. Christenhusz, J. W. Byng, The number of known plants species in the world and its annual increase. *Phytotaxa* **261**, 201–217 (2016).
3. Statista Research Department, Avocado industry—Statistics & facts. <https://www.statista.com/topics/3108/avocadoindustry/>. Accessed 29 July 2019.
4. Fresh Plaza, Mexico: Avocado exports generate 2.5 billion dollars. <https://www.freshplaza.com/article/178230/Mexico-Avocado-exports-generate-2.5-billion-dollars/>. Accessed 29 July 2019.
5. M. E. Galindo-Tovar, A. M. Arzate-Fernández, N. Ogata-Aguilar, I. Landero-Torres, The avocado (*Persea americana*, Lauraceae) crop in Mesoamerica: 10,000 years of history. *Harv. Pap. Bot.* **12**, 325–334 (2007).
6. B. A. Schaffer, B. N. Wolstenholme, A. W. Whitley, *The Avocado: Botany, Production and Uses* (CABI, 2013).
7. H. Chen, P. L. Morrell, V. E. Ashworth, M. de la Cruz, M. T. Clegg, Tracing the geographic origins of major avocado cultivars. *J. Hered.* **100**, 56–65 (2009).
8. S. Willingham *et al.*, Rootstock influences postharvest anthracnose development in 'Hass' avocado. *Aust. J. Agric. Res.* **52**, 1017–1022 (2001).
9. C. Illsley-Granich, R. Brokaw, S. Ochoa-Ascencio, "Hass Carmen, a precocious flowering avocado tree" in *Proceedings VII World Avocado Congress* (2011), pp. 5–9.
10. G. Furnier, M. Cummings, M. Clegg, Evolution of the avocados as revealed by DNA restriction fragment variation. *J. Hered.* **81**, 183–188 (1990).
11. F. A. Simão, R. M. Waterhouse, P. Ioannidis, E. V. Kriventseva, E. M. Zdobnov, BUSCO: Assessing genome assembly and annotation completeness with single-copy orthologs. *Bioinformatics* **31**, 3210–3212 (2015).
12. D. Kuhn *et al.*, Application of genomic tools to avocado (*Persea americana*) breeding: SNP discovery for genotyping and germplasm characterization. *Sci. Hortic. (Amsterdam)* **246**, 1–11 (2019).
13. T. H. Lee, H. Guo, X. Wang, C. Kim, A. H. Paterson, SNPPhylo: A pipeline to construct a phylogenetic tree from huge SNP data. *BMC Genomics* **15**, 162 (2014).
14. L. Skotte, T. S. Korneliusson, A. Albrechtsen, Estimating individual admixture proportions from next generation sequencing data. *Genetics* **195**, 693–702 (2013).
15. X. Zheng, B. S. Weir, Eigenanalysis of SNP data with an identity by descent interpretation. *Theor. Popul. Biol.* **107**, 65–76 (2016).
16. S. H. Martin, J. W. Davey, C. D. Jiggins, Evaluating the use of ABBA-BABA statistics to locate introgressed loci. *Mol. Biol. Evol.* **32**, 244–257 (2015).
17. M. Nei, W.-H. Li, Mathematical model for studying genetic variation in terms of restriction endonucleases. *Proc. Natl. Acad. Sci. U.S.A.* **76**, 5269–5273 (1979).
18. G. A. Watterson, On the number of segregating sites in genetical models without recombination. *Theor. Popul. Biol.* **7**, 256–276 (1975).
19. K. E. Holsinger, B. S. Weir, Genetics in geographically structured populations: Defining, estimating and interpreting F(ST). *Nat. Rev. Genet.* **10**, 639–650 (2009).
20. F. Tajima, Statistical method for testing the neutral mutation hypothesis by DNA polymorphism. *Genetics* **123**, 585–595 (1989).
21. E. Lyons, B. Pedersen, J. Kane, M. Freeling, The value of nonmodel genomes and an example using SynMap within CoGe to dissect the hexaploidy that predates the rosids. *Trop. Plant Biol.* **1**, 181–190 (2008).
22. V. A. Albert *et al.*, Amborella Genome Project, The Amborella genome and the evolution of flowering plants. *Science* **342**, 1241089 (2013).
23. H. Tang *et al.*, Unraveling ancient hexaploidy through multiply-aligned angiosperm gene maps. *Genome Res.* **18**, 1944–1954 (2008).
24. Y. Jiao *et al.*, A genome triplication associated with early diversification of the core eudicots. *Genome Biol.* **13**, R3 (2012).
25. O. Jaillon *et al.*, The grapevine genome sequence suggests ancestral hexaploidization in major angiosperm phyla. *Nature* **449**, 463–467 (2007).
26. C. Zheng, D. Santos Muñoz, V. A. Albert, D. Sankoff, Syntenic block overlap multiplicities with a panel of reference genomes provide a signature of ancient polyploidization events. *BMC Genomics* **16** (suppl. 10), S8 (2015).
27. C. Zheng, E. Chen, V. A. Albert, E. Lyons, D. Sankoff, Ancient eudicot hexaploidy meets ancestral eusoid gene order. *BMC Genomics* **14** (suppl. 7), S3 (2013).
28. M. J. Moore, C. D. Bell, P. S. Soltis, D. E. Soltis, Using plastid genome-scale data to resolve enigmatic relationships among basal angiosperms. *Proc. Natl. Acad. Sci. U.S.A.* **104**, 19363–19368 (2007).
29. D. E. Soltis *et al.*, Angiosperm phylogeny: 17 genes, 640 taxa. *Am. J. Bot.* **98**, 704–730 (2011).
30. D. E. Soltis *et al.*, Angiosperm phylogeny inferred from 18S rDNA, rbcL, and atpB sequences. *Bot. J. Linn. Soc.* **133**, 381–461 (2000).
31. N. J. Wickett *et al.*, Phylotranscriptomic analysis of the origin and early diversification of land plants. *Proc. Natl. Acad. Sci. U.S.A.* **111**, E4859–E4868 (2014).
32. D. Sankoff, C. Zheng, E. Lyons, H. Tang, "The trees in the peaks" in *International Conference on Algorithms for Computational Biology*, I. Holmes, C. Martin-Vide, M. A. Vega-Rodríguez, Eds. (Springer, 2016), pp. 3–14.
33. D. Sankoff *et al.*, Models for similarity distributions of syntenic homologs and applications to phylogenomics. *IEEE/ACM Trans. Comput. Biol. Bioinformatics* **10**, 1109/TCBB.2018.2849377 (2018).
34. L. Zeng *et al.*, Resolution of deep angiosperm phylogeny using conserved nuclear genes and estimates of early divergence times. *Nat. Commun.* **5**, 4956 (2014).
35. A. Hobolth, O. F. Christensen, T. Mailund, M. H. Schierup, Genomic relationships and speciation times of human, chimpanzee, and gorilla inferred from a coalescent hidden Markov model. *PLoS Genet.* **3**, e7 (2007).
36. D. A. Pollard, V. N. Iyer, A. M. Moses, M. B. Eisen, Widespread discordance of gene trees with species tree in *Drosophila*: Evidence for incomplete lineage sorting. *PLoS Genet.* **2**, e173 (2006).
37. J. B. Whitfield, P. J. Lockhart, Deciphering ancient rapid radiations. *Trends Ecol. Evol.* **22**, 258–265 (2007).
38. P. Librado, F. G. Vieira, J. Rozas, BadiRate: Estimating family turnover rates by likelihood-based methods. *Bioinformatics* **28**, 279–281 (2012).
39. D. Charlesworth, *Don't Forget the Ancestral Polymorphisms* (Nature Publishing Group, 2010).
40. G. I. Peterson, J. Masel, Quantitative prediction of molecular clock and ka/ks at short timescales. *Mol. Biol. Evol.* **26**, 2595–2603 (2009).
41. M. D. Rasmussen, M. Kellis, Unified modeling of gene duplication, loss, and coalescence using a locus tree. *Genome Res.* **22**, 755–765 (2012).
42. A. Suh, L. Smeds, H. Ellegren, The dynamics of incomplete lineage sorting across the ancient adaptive radiation of neoavian birds. *PLoS Biol.* **13**, e1002224 (2015).
43. M. Lynch, *The Origins of Genome Architecture* (Sinauer Associates, Sunderland, MA, 2007), vol. 98.
44. A. Force *et al.*, Preservation of duplicate genes by complementary, degenerative mutations. *Genetics* **151**, 1531–1545 (1999).
45. M. Freeling, Bias in plant gene content following different sorts of duplication: Tandem, whole-genome, segmental, or by transposition. *Annu. Rev. Plant Biol.* **60**, 433–453 (2009).
46. F. Cheng *et al.*, Gene retention, fractionation and subgenome differences in polyploid plants. *Nat. Plants* **4**, 258–268 (2018).
47. J. Salojärvi *et al.*, Genome sequencing and population genomic analyses provide insights into the adaptive landscape of silver birch. *Nat. Genet.* **49**, 904–912 (2017).
48. D. Beno-Moualem, D. Prusky, Early events during quiescent infection development by *Colletotrichum gloeosporioides* in unripe avocado fruits. *Phytopathology* **90**, 553–559 (2000).
49. C. H. Acosta-Muñoz *et al.*, Identification of avocado (*Persea americana*) root proteins induced by infection with the oomycete *Phytophthora cinnamomi* using a proteomic approach. *Physiol. Plant.* **144**, 59–72 (2012).
50. J. Engelbrecht, N. Van den Berg, Expression of defence-related genes against *Phytophthora cinnamomi* in five avocado rootstocks. *S. Afr. J. Sci.* **109**, 1–8 (2013).
51. E. Luna *et al.*, Callose deposition: A multifaceted plant defense response. *Mol. Plant Microbe Interact.* **24**, 183–193 (2011).
52. L. Eshraghi *et al.*, Phosphite primed defence responses and enhanced expression of defence genes in *Arabidopsis thaliana* infected with *Phytophthora cinnamomi*. *Plant Pathol.* **60**, 1086–1095 (2011).

53. N. v. d. Berg, J. B. Christie, T. A. S. Aveling, J. Engelbrecht, Callose and β -1,3-glucanase inhibit *Phytophthora cinnamomi* in a resistant avocado rootstock. *Plant Pathol.* **67**, 1150–1160 (2018).
54. J. Le Roy, B. Huss, A. Creach, S. Hawkins, G. Neutelings, Glycosylation is a major regulator of phenylpropanoid availability and biological activity in plants. *Front. Plant Sci.* **7**, 735 (2016).
55. N. D. Bonawitz, C. Chapple, The genetics of lignin biosynthesis: Connecting genotype to phenotype. *Annu. Rev. Genet.* **44**, 337–363 (2010).
56. C. L. Chang, I. K. Cho, Q. X. Li, Insecticidal activity of basil oil, trans-anethole, estragole, and linalool to adult fruit flies of *Ceratitis capitata*, *Bactrocera dorsalis*, and *Bactrocera cucurbitae*. *J. Econ. Entomol.* **102**, 203–209 (2009).
57. J. R. King, R. J. Knight, Occurrence and assay of estragole in the leaves of various avocado cultivars. *J. Agric. Food Chem.* **35**, 842–844 (1987).
58. X. Zhu et al., The wheat ethylene response factor transcription factor pathogen-induced ERF1 mediates host responses to both the necrotrophic pathogen *Rhizoctonia cerealis* and freezing stresses. *Plant Physiol.* **164**, 1499–1514 (2014).
59. L. Xing et al., Overexpression of ERF1-V from *Haynaldia villosa* can enhance the resistance of wheat to powdery mildew and increase the tolerance to salt and drought stresses. *Front. Plant Sci.* **8**, 1948 (2017).
60. I. Diniz et al., A first insight into the involvement of phytohormones pathways in coffee resistance and susceptibility to *Colletotrichum kahawae*. *PLoS One* **12**, e0178159 (2017).
61. W. F. Broekaert, S. L. Delauré, M. F. De Bolle, B. P. Cammue, The role of ethylene in host-pathogen interactions. *Annu. Rev. Phytopathol.* **44**, 393–416 (2006).
62. P. Lü et al., Genome encode analyses reveal the basis of convergent evolution of fleshy fruit ripening. *Nat. Plants* **4**, 784–791 (2018).
63. E. M. Yahia, A. B. Woolf, "Avocado (*Persea americana* Mill.)" in *Postharvest Biology and Technology of Tropical and Subtropical Fruits: Açai to Citrus*, E. Yahia, Ed. (Woodhead Publishing, 2011), pp. 125–186e.
64. L.-Á. Xoca-Orozco et al., Transcriptomic analysis of avocado hass (*Persea americana* Mill.) in the interaction system fruit-chitosan-Colletotrichum. *Front. Plant Sci.* **8**, 956 (2017).
65. N. L. Bray, H. Pimentel, P. Melsted, L. Pachter, Near-optimal probabilistic RNA-seq quantification. *Nat. Biotechnol.* **34**, 525–527 (2016).
66. W. Xu et al., Arabidopsis TCH4, regulated by hormones and the environment, encodes a xyloglucan endotransglycosylase. *Plant Cell* **7**, 1555–1567 (1995).
67. Y. Hu et al., Comparative transcriptome analysis unveils the tolerance mechanisms of *Citrus hystrix* in response to 'Candidatus Liberibacter asiaticus' infection. *PLoS One* **12**, e0189229 (2017).
68. N. H. Davila Olivas et al., Effect of prior drought and pathogen stress on Arabidopsis transcriptome changes to caterpillar herbivory. *New Phytol.* **210**, 1344–1356 (2016).
69. R. H. Tomas-Grau et al., Soft mechanical stimulation induces a defense response against *Botrytis cinerea* in strawberry. *Plant Cell Rep.* **37**, 239–250 (2018).
70. X. Wang et al., IDL6-HAE/HS2L impacts pectin degradation and resistance to *Pseudomonas syringae* pv *tomato* DC3000 in Arabidopsis leaves. *Plant J.* **89**, 250–263 (2017).